

A Xylosylphosphotransferase of *Cryptococcus neoformans* Acts in Protein O-Glycan Synthesis^{*[5]}

Received for publication, May 18, 2011. Published, JBC Papers in Press, May 23, 2011, DOI 10.1074/jbc.M111.262162

Morgann C. Reilly[‡], Kazuhiro Aoki[§], Zhuo A. Wang[‡], Michael L. Skowrya[‡], Matthew Williams[‡], Michael Tiemeyer[§], and Tamara L. Doering^{‡1}

From the [‡]Department of Molecular Microbiology, Washington University School of Medicine, St. Louis, Missouri 63110 and the [§]Complex Carbohydrate Research Center and Department of Biochemistry and Molecular Biology, University of Georgia, Athens, Georgia 30602

Cryptococcal meningoencephalitis is an AIDS-defining illness caused by the opportunistic pathogen *Cryptococcus neoformans*. This organism possesses an elaborate polysaccharide capsule that is unique among pathogenic fungi, and the glycobiology of *C. neoformans* has been a focus of research in the field. The capsule and other cellular glycans and glycoconjugates have been described, but the machinery responsible for their synthesis remains largely unexplored. We recently discovered Xpt1p, an enzyme with the unexpected activity of generating a xylose-phosphate-mannose linkage. We now demonstrate that this novel activity is conserved throughout the *C. neoformans* species complex, localized to the Golgi apparatus, and functions in the O-glycosylation of proteins. We also present the first survey of O-glycans from *C. neoformans*.

Members of the *Cryptococcus neoformans* species complex are the only organisms in the cryptococcal genus that are commonly associated with human disease. Historically categorized into four serotypes (A–D), these yeasts have more recently been classified into separate species and varieties: *C. neoformans* var. *grubii* (serotype A), *C. neoformans* var. *neoformans* (serotype D), and *Cryptococcus gattii* (serotypes B and C) (1). All four serotypes can be isolated from the environment, where they are most commonly found in association with avian excreta and soil (A and D) or certain tree species (B and C). Humans are infected via the inhalation of small yeast cells or basidiospores, which are typically neutralized within the lungs by the immune system without any symptomatic evidence of infection (2). In some instances, however, *C. neoformans* can disseminate from the lungs to other organs in the body; if it reaches the brain, it causes a fatal meningoencephalitis. Serotypes A and D are responsible for most infections of humans; they are generally associated with disease in immunocompromised individuals and have a worldwide distribution. In contrast, serotypes B and C characteristically infect immunocompetent populations and are typically found in tropical and subtropical regions, although

C. gattii is also responsible for an ongoing outbreak in the Pacific Northwest (3).

The capsule is the most distinctive structure of *C. neoformans*, and because it is required for virulence, has been intensively studied. This intricate structure is primarily composed of two polysaccharides, glucuronoxylomannan (GXM)² (4) and glucuronoxylomannogalactan (GXMGal) (5, 6). The capsule surrounds a cell wall composed of polymers of glucose, mannose, and *N*-acetyl-glucosamine, which are cross-linked to each other and to various highly glycosylated proteins. *Cryptococcus* species synthesize glycoproteins with extensive *N*- and *O*-linked modifications that may be comparable in mass to the protein itself (7–10); many of these bear glycosylphosphatidylinositol anchors (11–13) and are subsequently transferred to covalent linkage with the cell wall. The organism also synthesizes lipids modified with mannose, xylose, and galactose (14, 15). *C. neoformans* thus generates a broad array of cellular glycans and glycoconjugates that are only partially characterized. What we do know about their structures, however, indicates that they differ significantly from the glycan structures of their mammalian hosts as well as from related molecules in model yeasts.

We are interested in glycosyltransferases, enzymes that function in glycan synthesis by catalyzing the transfer of sugar moieties from activated donors (usually nucleotide sugars) to various acceptors (proteins, lipids, or other sugars). Previous studies of nucleotide sugar synthesis pathways in *C. neoformans* found that cells unable to produce UDP-xylose (UDP-Xyl) had no detectable Xyl residues in capsule polysaccharides, displayed shortened and deformed capsule fibers, and were avirulent in animal models of infection (16, 17). This physiological relevance of Xyl together with its frequent occurrence in cryptococcal glycoconjugates stimulated our interest in Xyl transfer activities. Using radiolabeled UDP-Xyl (UDP-[¹⁴C]Xyl) as the donor and α -1,3-linked dimannose (α -1,3-Man₂) as the acceptor in an *in vitro* assay of glycosyltransferase activities, we have characterized two xylosyltransferase reactions in *C. neoformans*. One of these is the transfer of Xyl from UDP-Xyl to the reducing Man of the disaccharide substrate, forming a β -1,2-linkage (18). This is mediated by either of two

^{*} This work was supported, in whole or in part, by National Institutes of Health Grants R01 GM071007 and R21 AI076737 (to T. L. D.) and P01 GM085354 and P41 RR018502 (National Center for Research Resources) (to M. T.).

^[5] The on-line version of this article (available at <http://www.jbc.org>) contains supplemental Fig. 1.

¹ To whom correspondence should be addressed: Dept. of Molecular Microbiology, Washington University School of Medicine, 660 South Euclid Ave., Campus Box 8230, St. Louis, MO 63110-1093. Tel.: 314-747-5597; Fax: 314-362-1232; E-mail: doering@wustl.edu.

² The abbreviations used are: GXM, glucuronoxylomannan; GXMGal, glucuronoxylomannogalactan; G418, Geneticin; NSI-MS, nanospray mass spectrometry; TIM, total ion mapping; ER, endoplasmic reticulum; Xyl, xylose; Xyl-P, xylose phosphate; α -1,3-Man₂, α -1,3-linked dimannose; YPD, yeast extract/peptone/dextrose.

TABLE 1
C. neoformans strains used in these studies

Name ^a	Serotype	Origin
KN99 α	A	Nielsen <i>et al.</i> (43)
KN99 α <i>xpt1</i> Δ	A	Reilly <i>et al.</i> (21)
KN99 α <i>xpt1</i> Δ p <i>XPT1</i>	A	Reilly <i>et al.</i> (21)
KN99 α <i>xpt1</i> Δ p <i>XPT1</i> -HA	A	Reilly <i>et al.</i> (21)
KN99 α <i>xpt1</i> Δ p <i>XPT1</i> (D)	A	This study
KN99 α <i>cap59</i> Δ	A	Baker <i>et al.</i> (44)
WM276	B	Warren <i>et al.</i> (45)
MMRL2651	C	Fraser <i>et al.</i> (46)
JEC21	D	Kwon-Chung <i>et al.</i> (47)
JEC21 p <i>XPT1</i>	D	This study
JEC21 p <i>XPT1</i> -HA	D	This study
JEC21 <i>GMT1</i> -HA	D	This study
JEC21 <i>GMT1</i> -HA p <i>XPT1</i>	D	This study
JEC21 <i>GMT1</i> -HA p <i>XPT1</i> -FLAG	D	This study

^a All strains are MAT α .

proteins: Cxt1p (18) and Cxt2p.³ Cxt1p acts in the synthesis of both of the capsule polysaccharides (GXM and GXMGal) and some cellular glycolipids (19, 20); less is known regarding the function of Cxt2p.

Besides the xylose addition that is mediated by the Cxt proteins, we have discovered a completely distinct and novel activity of *C. neoformans* that adds xylose-phosphate (Xyl-P) to Man-containing substrates (21). The resulting Xyl-P-Man linkage has not been previously observed in the glycan structures of *C. neoformans* or any other organism nor has an enzyme with xylosylphosphotransferase activity been described. We have identified and characterized the *C. neoformans* protein responsible for this activity, xylosylphosphotransferase 1 (Xpt1p (21)). This protein is specific for UDP-Xyl as the reaction donor but readily modifies a variety of Man-containing substrates. A significant gap in our knowledge is the biological function of Xpt1p. Although the moiety it forms has not been detected in the known glycolipid or capsule polysaccharide structures of *C. neoformans*, many glycan elements of the cell remain uncharacterized. Below, we describe our investigation into the function of Xpt1p and present evidence that this enzyme acts in the O-linked glycosylation of proteins.

EXPERIMENTAL PROCEDURES

Materials—UDP-[U-¹⁴C]xylose (UDP-[¹⁴C]Xyl; 151 mCi/mmol) was from PerkinElmer Life Sciences, and α -1,3-D-mannobiose (α -1,3-Man₂) was from Carbohydrate Synthesis (Oxford, UK). The murine monoclonal anti-GXM antibodies used were 3C2 and 339 (22), F12D2 (23), 1255 (24), and 1326 (25). Unless specified, all other chemicals or reagents were obtained from Sigma.

Strains, Plasmids, and Viability Testing—*C. neoformans* strains (Table 1) were grown in liquid culture at 30 °C in YPD medium (1% w/v yeast extract, 2% w/v peptone, 2% w/v dextrose) with shaking (230 rpm) or at 30 °C on YPD agar plates (YPD medium with 2% w/v agar). As appropriate, media included 100 μ g/ml nourseothricin (Werner BioAgents) and/or Geneticin[®] (G418; Invitrogen). For immunofluorescence localization, strains were cultured at 30 °C in minimal medium (0.17% yeast nitrogen base without amino acids, 2% w/v dextrose).

To test whether Xpt1 from serotype D complements the defect in a serotype A *xpt1* Δ strain, the coding sequence of the serotype D gene, designated here as *XPT1*(D), was PCR-amplified from JEC21 genomic DNA (prepared as described in Wickes *et al.* (26)) using primers MSPE-003 (CACCGCGCCCGCCCCGAAAATGCCGCCGACCGCGCTGC) and MSPE-004 (CTCCTTCTACGTTCTATGTCTAGTCATGATATCTGTCTTTTACAGG). Regions flanking the serotype A *XPT1* gene were PCR-amplified from the plasmid p*XPT1* (21) using primers MSPE-001 (GCTCAGTGTCTCGCATATGGT) and MSPD-002 (GCTGCAGGAATTCGATATCAAGC) for the upstream sequence and primers MSPD-005 (GCTCTCCAGCTCACATCCTCGCAGCGTTTCGAGAGTTGCTTTTTCACGG) and MSPE-006 (CTTACAACGGCTGGTACTCTGG) for the downstream sequence. The three amplicons (upstream sequence, coding region, and downstream sequence) were next assembled by three-way fusion PCR using primers MSPE-001 and MSPE-006, and the resulting product was digested with HpaI and NheI and cloned into p*XPT1* that had been digested with HpaI and NheI and treated with calf intestinal alkaline phosphatase. The resulting p*XPT1*(D) plasmid, differing from p*XPT1* only in the *XPT1* coding sequence, was transformed into DH5 α *Escherichia coli* cells, isolated, linearized with I-SceI, and transformed into the *C. neoformans* strain KN99 α *xpt1* Δ by electroporation (26). G418-resistant transformants were screened by PCR for the presence of serotype D *XPT1* sequence, and positive clones were assayed for xylosyltransferase activity.

For some experiments an Xpt1p overexpression strain was used. This was generated by transforming p*XPT1* linearized with I-SceI into KN99 α by electroporation and selecting and maintaining transformants in YPD containing 100 μ g/ml G418.

To test *C. neoformans* viability under various growth conditions, cells from an overnight culture were washed in water and adjusted to 2×10^6 cells/ml; 5 μ l (10^4 cells) of this suspension and of four 10-fold serial dilutions were spotted on YPD agar or YPD stressor plates (YPD agar with 0.5 mg/ml caffeine, 0.05% sodium dodecyl sulfate (SDS), 1 mM sodium nitrite, or 0.5 mM hydrogen peroxide) and then incubated at 30 °C or 37 °C.

Total Membrane Preparation and Detergent Extraction—*C. neoformans* membranes and their detergent extracts were prepared as in Reilly *et al.* (21). Briefly, cells from an overnight culture were washed in Tris-EDTA buffer (100 mM Tris-HCl, pH 8.0, 0.1 mM EDTA) and broken with glass beads, and the resulting lysate was subjected to a clearing centrifugation step. Total membranes were isolated from the resulting supernatant fraction by ultracentrifugation, resuspended in Tris buffer (100 mM Tris-HCl, pH 8.0), and stored at 4 °C. Protein concentration of the total membrane sample was determined using the Bio-Rad Protein Assay. For some studies, membranes were extracted with 1% Triton X-100 and subjected to a second round of ultracentrifugation, and the resulting supernatant fraction was stored at 4 °C. Protein concentration of the Triton X-100 extract sample was determined using the Bio-Rad Detergent Compatible Protein Assay.

Xylosyltransferase Activity Assays—Enzyme activity was assayed by monitoring the transfer of [¹⁴C]Xyl from a UDP-[¹⁴C]Xyl donor to an α -1,3-Man₂ acceptor as in (21). Briefly, reactions containing 625 μ g of protein (from *C. neoformans*

³ J. S. Klutts and T. L. Doering, manuscript in preparation.

Function of a *Cryptococcal* Xylosylphosphotransferase

total membranes or Triton X-100 extracts), 1 μM UDP-[^{14}C]Xyl, 8.8 mM α -1,3-Man₂, and 7.5 mM MnCl₂ in 100 mM Tris-HCl, pH 6.5, were incubated overnight at 20 °C. Unreacted UDP-Xyl was removed with anion exchange resin, and the reaction products were resolved by thin layer chromatography (TLC) and visualized by autoradiography.

Growth in Mice—For each strain tested, eight 4–6-week-old female C57Bl/6 mice (The Jackson Laboratory) were anesthetized with a combination of Ketaset-HCl and xylazine and inoculated intranasally with 50 μl of a 2.5×10^5 cells/ml suspension in phosphate-buffered saline, pH 7.4 (PBS). Three animals from each cohort were sacrificed at 1 h post-inoculation; the remaining five were sacrificed at 7 days post-inoculation. After sacrifice, lungs were harvested and homogenized in PBS, and serial dilutions of the homogenate were plated on YPD agar for determination of colony-forming units. Initial inocula were also plated to confirm colony-forming units.

Capsule Staining—Cells from an overnight culture of *C. neoformans* were washed twice with PBS, resuspended at 10^7 cells/ml in PBS containing 1% bovine serum albumin (PBS + 1% BSA), and rotated for 1 h at room temperature with a final concentration of 8 $\mu\text{g/ml}$ anti-GXM antibody. Cells were washed twice with PBS and then incubated for 1 h at room temperature with rotation in PBS + 1% BSA containing 3.2 $\mu\text{g/ml}$ Alexa Fluor[®] 546 goat anti-mouse IgG (Invitrogen). Cells were again washed twice with PBS and suspended in PBS for visualization. Bright field and fluorescence images were acquired simultaneously on a Zeiss Axioskop 2 MOT Plus wide-field fluorescence microscope; all samples were imaged with identical acquisition settings.

Capsule Induction—Cells from an overnight culture of *C. neoformans* were resuspended at 10^5 cells/ml in 50 ml of YPD media plus appropriate antibiotics and again cultured overnight. The subcultured cells were resuspended at 10^7 cells/ml in 10 ml of Dulbecco's modified Eagle's medium, transferred to a 25-cm² tissue culture flask, and incubated at 37 °C with 5% CO₂ for 20 h. 1 ml of cells was harvested, washed once with water, and resuspended in 100 μl of India ink for visualization. Bright field images were acquired on a Zeiss Axioskop 2 MOT Plus wide-field fluorescence microscope as above.

Lipid Glycosylation—Reactions of 625 μg of total membrane protein, 1 μM UDP-[^{14}C]Xyl, and 7.5 mM MnCl₂ in 100 mM Tris-HCl, pH 6.5, were incubated overnight at 20 °C. Chloroform and methanol were added for a final ratio of 10:10:3 (chloroform:methanol:buffer); the resulting mixture was incubated for 30 min at room temperature with occasional vortex mixing and then centrifuged to remove particulate material (16,000 \times g; 2 min). The supernatant fraction was transferred to a fresh tube and dried under a stream of nitrogen gas. The sample was then resuspended in *n*-butanol, vortexed with an equal volume of water, and centrifuged as before, and the resulting organic phase was transferred to a fresh tube. The remaining aqueous phase was again extracted with an equal volume of *n*-butanol, and the pooled organic phases were washed with an equal volume of water, transferred to a fresh tube, and dried as before. The sample was resuspended in 1:1 methanol:water, applied to a Silica Gel 60 plate (EM Sciences), and resolved by TLC in a solvent system of 10:10:3 chloroform:methanol:water. The

dried plate was sprayed with En³Hance[®] Spray (PerkinElmer), and radiolabeled products were visualized by autoradiography.

Protein Glycosylation—Xylosyltransferase reactions were performed as in the previous section. After overnight incubation, some reactions were treated with 1 unit of Protease Type XIV (from *Streptomyces griseus*) or a buffer control (0.01 M sodium acetate, 0.005 M calcium acetate, and 0.01 M CaCl₂) for 24 h at 37 °C. All samples were mixed with sample buffer, heated for 15 min at 100 °C, and resolved by SDS-PAGE on a 10% gel according to standard methods (27). The gel was fixed for 1 h in 5:4:1 methanol:water:acetic acid, incubated in Enlightning Rapid Autoradiography Enhancer (PerkinElmer) for 30 min, dried onto 3MM chromatography paper (Whatman), and visualized by autoradiography.

Preparation of Protein-linked Glycans for Analysis—A 50-ml overnight culture of *C. neoformans* was used to inoculate 1 liter of YPD with or without 100 $\mu\text{g/ml}$ G418 at 10^5 cells/ml. The sub-cultured cells were grown for 24 h (to $\sim 10^7$ cells/ml), harvested by centrifugation, and washed with Tris-EDTA buffer. Cells were resuspended in 10 ml of the same buffer and disrupted with glass beads, and the resulting lysate was subjected to a clearing centrifugation step as described in Reilly *et al.* (21) for the preparation of membrane proteins. The supernatant fraction was transferred to a fresh tube, and CHAPS was added to a final concentration of 1%; the sample was incubated at 4 °C with rocking for 2 h and then subjected to ultracentrifugation (75,000 \times g; 45 min). The detergent-soluble fraction was transferred to cellulose dialysis tubing (8000 M_r cut-off; from Fisher) and dialyzed against 2 liters of 50 mM ammonium bicarbonate buffer at 4 °C; the buffer was changed every 12 h for a total of 8 liters over 48 h. The dialyzed sample was transferred to a 50-ml conical tube, frozen at -80 °C, and lyophilized. The lyophilized protein material was washed by precipitation using ice-cold 80% acetone to reduce residual detergent and other polymeric contaminants that can interfere with mass spectrometric detection (a polyhexose ladder of unknown origin, also observed in similar analyses of non-cryptococcal samples, remains at low levels and is indicated on spectra below). Protein content of the washed, lyophilized material was determined by BCA assay to be 169 ± 42 or 198 ± 27 μg of protein/mg of lyophilized material for KN99 α or KN99 α *xpt1* Δ , respectively ($n = 3$).

Oligosaccharides were released from the *C. neoformans* samples by reductive β -elimination as detailed in Aoki *et al.* (28). Briefly, the lyophilized *C. neoformans* material (2.5 mg) was resuspended in a solution of 100 mM sodium hydroxide and 1 M sodium borohydride and incubated for 18 h at 45 °C. The reaction mixture was neutralized with 10% acetic acid on ice and then loaded onto a column of AG 50W-X8 cation-exchange resin (Bio-Rad) for desalting. The column run-through and a subsequent wash with three bed volumes of 5% acetic acid, both containing released oligosaccharides, were combined and lyophilized to dryness. To remove borate from the sample, a solution of 10% acetic acid in methanol was added, and the sample was then dried under a stream of nitrogen gas at 37 °C; this was repeated for a total of 5 times. The sample was then resuspended in 5% acetic acid and loaded onto a C18 cartridge column (Mallinckrodt Baker) that was previously washed with

acetonitrile and pre-equilibrated with 5% acetic acid. Flow-through from the column was collected after loading; the column was then washed a total of five times with 5% acetic acid. The flow-through and washes were combined and evaporated to dryness.

Analysis of Glycans by Nanospray Ionization Mass Spectrometry (NSI-MSⁿ)—Samples were analyzed as in Aoki *et al.* (28). Briefly, the released oligosaccharide sample was permethylated (29), dissolved in 1 mM sodium hydroxide in 50% methanol, and infused into a linear ion trap mass spectrometer equipped with an Orbitrap FT detector (LTQ-Orbi Discoverer, Thermo-Fisher). MS analysis was performed in positive ion mode. The total ion mapping (TIM) function of the Xcalibur software package (Thermo-Fisher) was utilized to detect and quantify the prevalence of individual glycans in the total glycan profile; peaks were considered quantifiable if they were 2-fold or greater above background. The generation of TIM profiles includes automated acquisition of MS/MS spectra in overlapping collection windows ($\Delta m/z = 2.8$ mass units, window-to-window overlap set at 0.8 mass units) across user-defined mass ranges (generally from $m/z = 200$ –2000). These fragmentation spectra highlighted the presence of cryptococcal glycans at particular m/z values, providing guidance for subsequent experiments in which glycans of interest were manually fragmented (MSⁿ) to assign structure.

Protein Localization—pXPT1-FLAG, a construct for the expression of a C-terminal FLAG-tagged Xpt1p, was generated exactly as pXPT1-HA (described in Reilly *et al.* (21)) except that primers MCR136 (TTACTTGTTCATCGTCATCCTTGTAAATCATCATTATACCTATCTTTTACAGGATCCC) and MCR137 (GATTACAAGGATGACGATGACAAGTAAACATAGAACGTAGAAGGAGATGGAGG) were used in place of MCR120 and MCR121, respectively. The pXPT1-HA or pXPT1-FLAG plasmids were linearized with I-SceI and transformed into the *C. neoformans* strain JEC21 by electroporation (26), and transformants were selected by growth on G418 plates.

Cells were cultured overnight in minimal medium (final density $\sim 10^8$ cells/ml), mixed with formaldehyde (4% final), and incubated for 30 min at 30 °C with shaking. All subsequent steps were performed at room temperature. Cells (4×10^8) were harvested by centrifugation ($400 \times g$; 1 min), washed once with PBS, resuspended in 1 ml of a fresh solution of 4% formaldehyde in PBS, and incubated for 30 min with rotation. The sample was then washed 3 times with PBS, resuspended in 1 ml of lysis buffer (50 mM sodium citrate pH 6.0, 1 M D-sorbitol, 35 mM β -mercaptoethanol) plus 25 mg/ml Lysing Enzymes (from *Trichoderma harzianum*), and incubated for 1 h at 30 °C with occasional inversion. After digestion, the cells were washed twice with HS Buffer (100 mM HEPES, pH 7.5, 1 M D-sorbitol) and resuspended in 200 μ l of HS Buffer.

The washed cell suspension was spotted in 20- μ l aliquots on a glass microscope slide coated with 0.1% poly-L-lysine and incubated for 20 min at room temperature, and the buffer was removed by aspiration. All subsequent treatments and washes were performed by the application of 20- μ l volumes and incubation at room temperature and were followed by aspiration. The slides were first treated with HS Buffer containing 1% Tri-

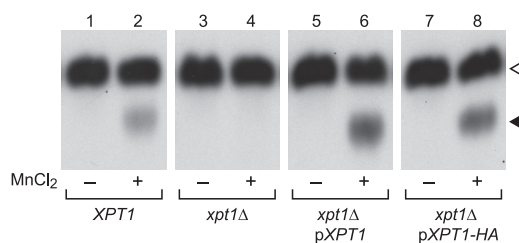


FIGURE 1. Xylosyltransferase activities in *C. neoformans*. Total membranes prepared from wild-type KN99 α (*XPT1*), mutant (*xpt1* Δ), or episomally-complemented mutant (*xpt1* Δ p*XPT1* and *xpt1* Δ p*XPT1*-HA) strains were assayed with UDP-[¹⁴C]Xyl and α -1,3-Man₂ in the absence (–) or presence (+) of MnCl₂, as described under “Experimental Procedures.” An autoradiograph of the products resolved by TLC is shown; no signal was detected in other regions of the plate beyond minor amounts of free Xyl. The filled triangle indicates the product of the manganese-dependent xylosyltransferase activity, and the open triangle indicates the product of the unrelated xylosyltransferase Cxt1p (see “Results”). No signal was detected in the absence of the α -1,3-Man₂ acceptor (not shown).

ton X-100 and incubated for 10 min; they were then washed 3 times with HS Buffer and 3 times with PBS. The slides were next treated with Blocking Buffer (5% goat serum, 0.02% Triton X-100 in PBS) for 1 h followed by either a high affinity rat anti-HA monoclonal antibody (20 ng/ml in Blocking Buffer; from Roche Applied Science) or Blocking Buffer alone overnight in a moist chamber at 4 °C. Samples were then washed six times with Blocking Buffer and stained with Alexa Fluor[®] 594 goat anti-rat IgG (1 μ g/ml in Blocking Buffer; from Invitrogen) for 1 h in the dark; next, slides were washed 6 times with Blocking Buffer, 3 times with PBS, and then stained with DAPI (5 μ g/ml in PBS) for 30 min in the dark. Finally, samples were washed three times with PBS and allowed to air-dry. Prolong Gold was applied to each sample followed by a glass coverslip, and the slide was stored for less than 24 h at –20 °C in the dark. Bright field and fluorescence images were acquired as for the capsule staining assays above.

RESULTS

Xylosyltransferases in *C. neoformans*—We have identified several xylosyltransferase activities in *C. neoformans* by assaying the transfer of radiolabeled Xyl from the nucleotide sugar donor UDP-[¹⁴C]Xyl to an α -1,3-Man₂ oligosaccharide acceptor (see “Experimental Procedures”). When membranes prepared from the wild-type strain KN99 α were used as the source of enzyme activity in this assay, two distinct products were observed (Fig. 1, track 2). The upper product (open arrowhead) is Xyl-linked β -1,2 to the reducing Man of the α -1,3-Man₂ substrate (18); this is synthesized primarily by Cxt1p, which generates a Man- α (1 \rightarrow 3)[Xyl- β (1 \rightarrow 2)]-Man motif that occurs in one of the major cryptococcal glycosylinositol phosphorylceramides, GXM, and GXMGal (19, 20). The lower product (closed arrowhead) is Xyl-P-linked to the non-reducing Man of α -1,3-Man₂, a completely novel linkage that is generated by Xpt1p (21). Strains in which *XPT1* has been replaced with a drug resistance cassette no longer generate this product (Fig. 1, track 4), a defect that can be complemented by the episomal expression of *XPT1* (Fig. 1, track 6; Ref. 21). Modifying the episomal copy to incorporate an HA epitope tag at the protein C-terminus does not alter enzyme activity in this assay (Fig. 1, track 8).

We began our investigation into the biological function of Xpt1p by exploring its conservation among members of the

Function of a Cryptococcal Xylosylphosphotransferase

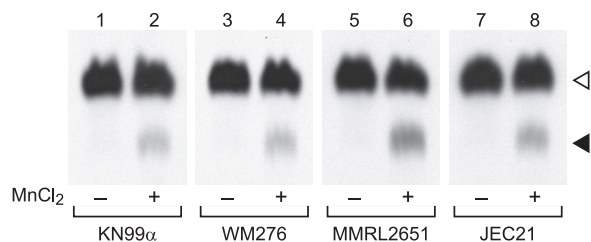


FIGURE 2. Xpt1p activity in members of the *C. neoformans* species complex is comparable. Total membranes prepared from the indicated strains were assayed with UDP- ^{14}C Xyl and α -1,3-Man $_2$ in the absence (–) or presence (+) of MnCl $_2$, as described under “Experimental Procedures.” An autoradiograph of the products resolved by TLC is shown; no signal was detected in other regions of the plate beyond minor amounts of free Xyl. The filled triangle indicates the product of the manganese-dependent xylosyltransferase activity, and the open triangle indicates the product of the unrelated xylosyltransferase Cxt1p (see “Results”). No signal was detected in the absence of the α -1,3-Man $_2$ acceptor (not shown).

C. neoformans species complex, which differ in terms of ecological niche, host preference, and disease outcome (1). To do this, we performed xylosyltransferase activity assays on membranes prepared from cryptococcal strains representing the four major historically defined serotypes: A (KN99 α , H99), B (WM276, R265), C (NIH312, MMRL2751), and D (JEC21, KN355 α , KN433 α). In each strain tested, we observed a xylosylated species that co-migrated with the Xpt1p product made by KN99 α membranes and was similarly manganese-dependent (Fig. 2 and data not shown). These results were consistent with our identification of sequences homologous to the serotype A *XPT1* (locus *CNAG_04860*, from the *C. neoformans* var. *grubii* H99 data base maintained by the Broad Institute) in the genomes of serotypes B (locus *CNGB_5687*; from the *C. gattii* R265 data base maintained by the Broad Institute) and D (locus *CNJ02890*; from the *C. neoformans* var. *neoformans* JEC21 data base maintained by TIGR).⁴

We next investigated whether the *XPT1* sequence from one serotype could complement deletion of the native *XPT1* from another. Membranes from serotype A *xpt1* Δ cells, which exhibit no Xpt1p activity (Fig. 3, track 4) acquired activity upon episomal expression of the serotype D gene (Fig. 3, track 8). This activity was equal to that conferred by expression of the native serotype A gene from the same plasmid backbone (Fig. 3, track 6). Xylosylphosphotransferase activity in the mutant strain complemented with either plasmid exceeded that of wild-type cells (Fig. 3, track 2), likely due to the presence of multiple copies of the plasmids.

Growth of *xpt1* Δ Strains—We next assessed the basic growth characteristics of cells deleted for *XPT1* (*xpt1* Δ) compared with wild-type. Cultures of KN99 α and KN99 α *xpt1* Δ grew comparably in liquid and on solid rich medium; this held true at both 30 °C (the optimal growth temperature for *C. neoformans*) and 37 °C (data not shown). Similar results were obtained when the plate medium was supplemented with caffeine, SDS, sodium nitrate, or hydrogen peroxide, which act as cell wall, cell membrane, nitrosative, and oxidative stressors, respectively (data not shown). We also compared the growth of KN99 α and KN99 α *xpt1* Δ in a mouse model of cryptococcal infection. The levels of colony-forming units recovered from the lungs of mice

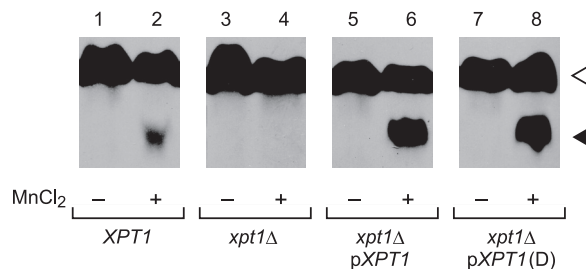


FIGURE 3. Expression of *XPT1* from serotypes A and D similarly complements the serotype A *xpt1* Δ mutant. Total membranes prepared from serotype A wild-type (*XPT1*), serotype A *xpt1* Δ (*xpt1* Δ), serotype A *xpt1* Δ cells expressing *XPT1* from the same serotype (*xpt1* Δ p*XPT1*), and serotype A *xpt1* Δ cells expressing *XPT1* from serotype D (*xpt1* Δ p*XPT1* (D)) were assayed with UDP- ^{14}C Xyl and α -1,3-Man $_2$ in the absence (–) or presence (+) of MnCl $_2$, as described under “Experimental Procedures.” An autoradiograph of the products resolved by TLC is shown; no signal was detected in other regions of the plate beyond minor amounts of free Xyl or in the absence of the α -1,3-Man $_2$ acceptor (not shown). The filled triangle indicates the product of the manganese-dependent xylosyltransferase activity, and the open triangle indicates the product of the unrelated xylosyltransferase Cxt1p (see “Results”).

after intranasal inoculation were the same for the wild-type and deletion strains (data not shown). Collectively, these studies indicated that the loss of Xpt1p did not influence growth or viability under the conditions tested, but they gave no indication of its cellular function.

Potential Roles of Xpt1p—We examined the potential role of Xpt1p in capsule formation by comparing the capsule morphologies of KN99 α , KN99 α *xpt1* Δ , and KN99 α *xpt1* Δ complemented with the native gene on a plasmid (p*XPT1*). We first assessed the binding of monoclonal anti-GXM antibodies to the cell surface. Each of the antibodies tested (see “Experimental Procedures”) demonstrated uniform staining around the cell periphery (shown for antibody F12D2 in supplemental Fig. 1, panel A), indicating no obvious alteration in the mutant strain at the level of immunofluorescence microscopy. We also tested the ability of mutant strains to increase the radius of their capsule in response to “inducing” growth conditions (30). Both the KN99 α and KN99 α *xpt1* Δ strains enlarged the capsule to a comparable extent (supplemental Fig. 1, panel B). For comparison, an acapsular control strain, *cap59* Δ , showed no capsule staining or induction (supplemental Fig. 1).

Prior studies of capsule polysaccharides did not indicate the presence of Xyl-P in GXM or GXMGal (4–6). To confirm this finding, ^{31}P NMR analysis was performed on GXM prepared from KN99 α ; no phosphate signal was detected in this analysis (data not shown).⁵ As this absence is consistent with the lack of capsule alteration in *xpt1* Δ mutant cells, we did not pursue additional analysis of capsule polysaccharides in the mutant.

We next considered that Xpt1p might participate in the xylosylation of cryptococcal glycolipids. To test this we performed reactions similar to our standard xylosyltransferase assay, but lacking the α -1,3-Man $_2$ substrate such that only endogenous compounds were available as acceptor molecules. Membrane preparations from wild-type, mutant, and complemented strains (KN99 α , KN99 α *xpt1* Δ , and KN99 α *xpt1* Δ p*XPT1*) were assayed in this manner, and the lipids were then extracted from the radiolabeled samples for analysis by TLC. Although we

⁴ Genome sequence from a serotype C strain is not currently available.

⁵ C. Heiss, personal communication.

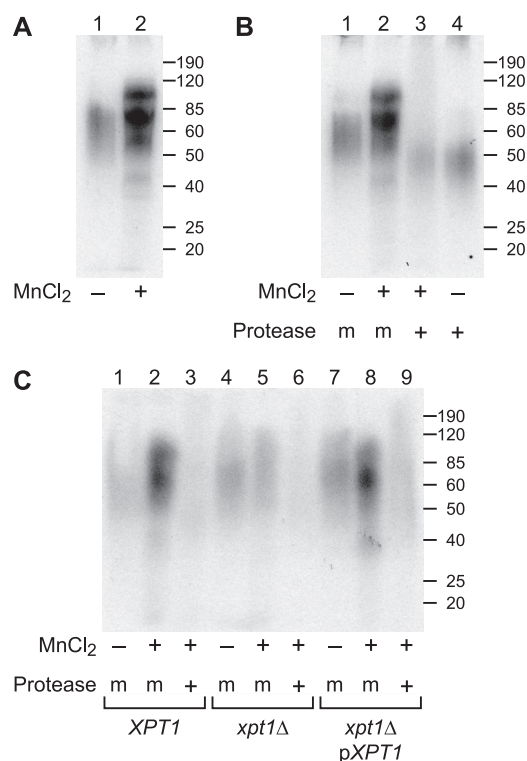


FIGURE 4. Protein glycosylation studies of *xpt1Δ* mutant. Total membranes prepared from the indicated strains were assayed with UDP- ^{14}C Xyl in the presence (+) or absence (–) of MnCl_2 as indicated; some samples were subsequently mock-treated (*m*) or treated with protease (+) as indicated. *Panel A* shows manganese stimulation of radiolabel incorporation. *Panel B* shows protease degradation of assay products. *Panel C* shows Xpt1p dependence of radiolabel incorporation. Autoradiographs of dried SDS-PAGE gels are shown. Molecular weight standards (in kDa) are indicated at the right.

detected the incorporation of ^{14}C Xyl into several lipid species, this activity was not dependent on the presence of Xpt1p (data not shown). These data indicated that Xpt1p does not act in glycolipid synthesis.

We speculated that another potential role for Xpt1p was in protein glycosylation. Similar to the lipid experiment outlined above, we incubated cryptococcal membranes with UDP- ^{14}C Xyl (but not α -1,3- Man_2) and then analyzed the samples by SDS-PAGE. KN99 α membranes assayed in this manner incorporated ^{14}C Xyl into material that migrated between 50 and 100 kDa (Fig. 4, *panel A*). Notably, the observed incorporation of ^{14}C Xyl increased significantly upon the addition of MnCl_2 to the reactions, indicating that some xylosylation was due to a manganese-dependent activity (Fig. 4, *panel A*, compare *lanes 1* and *2*). Protease treatment of these assay products reduced the ^{14}C Xyl signal relative to mock-digested controls, demonstrating that the radiolabel was indeed associated with a polypeptide species (Fig. 4, *panel B*).

Although ^{14}C Xyl-labeling of protein in KN99 α membranes was clearly stimulated by the addition of MnCl_2 , this could have been due to synthetic activities of enzymes other than Xpt1p. To test this, we performed similar experiments with membrane preparations from KN99 α , KN99 α *xpt1Δ*, and KN99 α *xpt1Δ* pXPT1 cells. The intensity and pattern of radiolabel incorporation was comparable for both the wild-type and complemented strains (Fig. 4, *panel C*, *lanes 1–3* and *lanes 6–9*); in both strains, the inclusion of MnCl_2 increased ^{14}C Xyl incorporation and

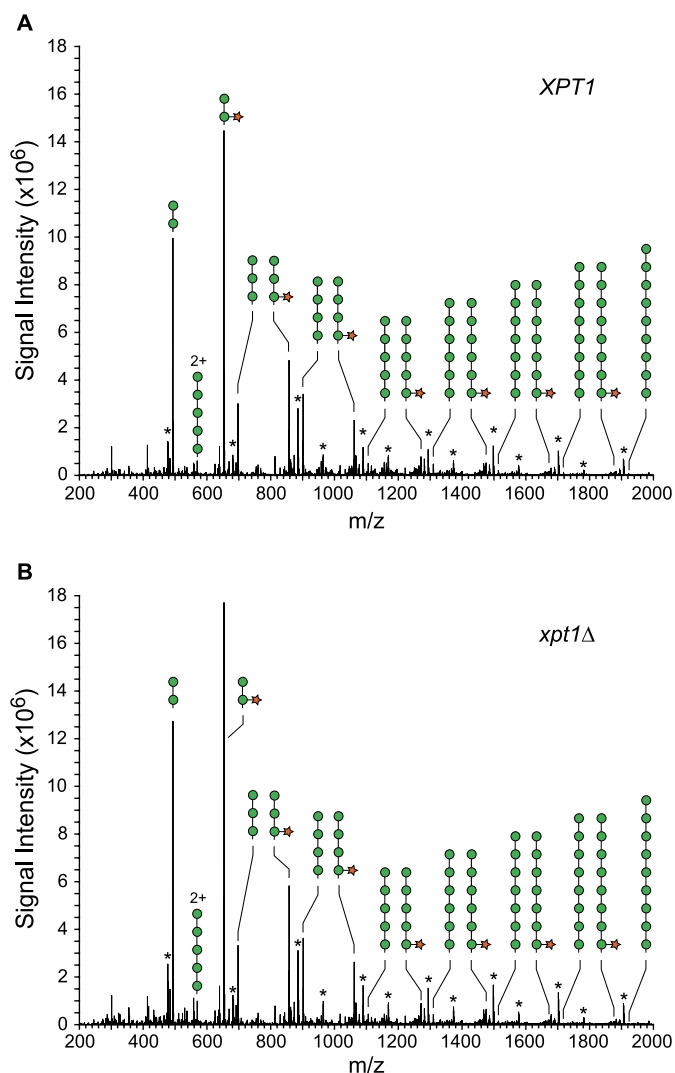


FIGURE 5. The profiles of major O-linked glycans released from wild-type and *xpt1Δ* mutant proteins are similar. Full MS scans are shown for glycans released from equivalent amounts of protein harvested from wild-type KN99 α (*panel A*) and the KN99 α *xpt1Δ* mutant (*panel B*). Man_n and Xyl-Man_n glycans dominate the O-linked glycan profile. Asterisks denote the presence of a poly-hexose contaminant of unknown origin (non-reduced). 2+ denotes double-charged ion species; circle, Man ; star, Xyl .

protease treatment of the reaction products significantly reduced the resulting ^{14}C Xyl-labeling. In contrast, membranes from the KN99 α *xpt1Δ* strain showed no increase in protein radiolabeling upon the addition of MnCl_2 (Fig. 4, *panel C*, *lanes 4–6*). These studies strongly implicated Xpt1p in protein glycosylation.

Analysis of O-Linked Glycans—Based on our radiolabeling studies, we next turned to direct analysis of protein-associated glycans. Total cell lysates were prepared from KN99 α and KN99 α *xpt1Δ* cells and extracted with 1% CHAPS; O-glycans were then released from the detergent-soluble material by β -elimination, permethylated, and analyzed by NSI-MS (see “Experimental Procedures”). The major species of O-linked glycans in both the wild-type and *xpt1pΔ* samples were similar in distribution and were consistent with structures of Man_2 , Man_3 , Man_4 , and their corresponding xylosylated forms: Xyl-Man_2 , Xyl-Man_3 , and Xyl-Man_4 (Fig. 5). MS^2 verified the pres-

Function of a Cryptococcal Xylosylphosphotransferase

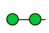
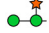
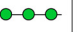








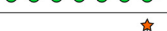






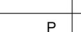

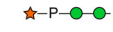
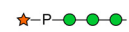

Structure	Predicted Mass	Percent of Total Profile	Structure	Predicted Mass	Percent of Total Profile
Man_n-O- Type			Xyl-Man_n-O- Type		
Man ₂ 	493.3	30.2	Xyl-Man ₂ 	653.3	13.3
Man ₃ 	697.4	12.1	Xyl-Man ₃ 	857.4	3.2
Man ₄ 	901.5	16.4	Xyl-Man ₄ 	1061.5	1.4
Man ₅ 	1105.6	4.2	Xyl-Man ₅ 	1265.5	0.3
Man ₆ 	1309.7	4.0	Xyl-Man ₆ 	1469.7	0.5
Man ₇ 	1513.8	2.3	Xyl-Man ₇ 	1673.8	0.1
Man ₈ 	1717.9	2.1	Xyl-Man ₈ 	1877.9	0.1
Man ₉ 	1922.0	1.7	Xyl-Man ₉ 	2082.0	0.1
Phosphomonoester Man_n-O- Type			Phosphomonoester Xyl-Man_n-O- Type		
P-Man ₂ 	587.2	<0.1	P-(Xyl)-Man ₂ 	747.3	<0.1
P-Man ₃ 	791.3	<0.1	P-(Xyl)-Man ₃ 	951.4	<0.1
			Phosphodiester-linked Xyl Type		
			Xyl-P-Man ₂ 	747.3	<0.1
			Xyl-P-Man ₃ 	951.4	<0.1
			Xyl-P-Man ₄ 	1155.5	<0.1

FIGURE 6. The mass and prevalence of individual O-linked glycans detected in detergent-extracts of *C. neoformans*. Protein samples for glycan analysis were prepared from KN99 α cells as described under "Experimental Procedures." After release from protein material by reductive β -elimination, alditols were permethylated and characterized by NSI-MSⁿ as their sodiated structures. Monoisotopic m/z values are given for the permethylated alditol forms of the indicated structures. The prevalence of each glycan is expressed as a percent of the total O-linked glycan profile quantified by measuring signal intensities from full MS spectra. Prevalence values are determined from complete TIM analysis of a single KN99 α extract. A prevalence value of <0.1% of total profile indicates that the glycan was detected and characterized by MSⁿ but was present at a level below the threshold for quantification (less than two times background).

ence of Man_n and Xyl-Man_n glycans extended to $n = 9$. The O-glycans of *C. neoformans*, which have not previously been comprehensively surveyed, also include minor glycans with properties consistent with being Man₂ or Man₃ cores carrying branching phosphomonoesters with or without Xyl (Fig. 6).

To investigate the potential occurrence of terminal Xyl-P phosphodiester motifs among the minor O-glycans, TIM data were filtered to reveal parent ions that produce MS² fragments corresponding to the loss of terminal Xyl ($\Delta m/z = 175$) or Xyl-1-P ($\Delta m/z = 285$). This analysis revealed the presence of low abundance O-glycans with terminal Xyl-1-P at $m/z = 747.3$ (Xyl-P-Man₂), $m/z = 951.4$ (Xyl-P-Man₃), and $m/z = 1155.5$ (Xyl-P-Man₄) (Fig. 6). Subsequent MSⁿ fragmentation in the wild-type KN99 α sample supported these structural assignments and unambiguously placed the Xyl-P- substitution on the non-reducing terminal Man residue of the glycan (Fig. 7). We next examined O-glycans from *xpt1* Δ cells for the presence of these moieties. Extremely low signal intensities were detectable within TIM collection windows of $\Delta m/z \pm 1.4$ mass units centered around $m/z = 748$ and $= 952$ for *xpt1* Δ glycans (Fig. 8, left profiles). Based on signal intensities in full MS, the reduction in the Xyl-P-Man₂ glycan relative to KN99 α wild type was between 12- and 20-fold (data from two independent prepara-

tions). Fragmentation associated with $m/z = 952$ (Xyl-P-Man₃) and $m/z = 1155$ (Xyl-P-Man₄) failed to yield interpretable spectra in the *xpt1* Δ glycans, indicating reduction below the threshold for detection.

To confirm the relationship between the Xpt1p activity and Xyl-P-modified O-glycans, we analyzed cells expressing increased levels of the transferase. To do this we exploited our observation that episomal expression of Xpt1p increased enzyme activity severalfold over wild-type levels (Fig. 3) and expressed *XPT1* in *xpt1* Δ cells from a plasmid marked with a sequence conferring resistance to G418. Membranes prepared from the resulting strain grown in medium containing G418 showed a 3.5-fold increase in xylosylphosphotransferase activity compared with wild-type cells in which *XPT1* is expressed only from its native chromosomal location (Fig. 9A, compare tracks 4 and 2). This activity declined when the plasmid-bearing cells were grown in medium lacking G418 for 24 h, consistent with the expected plasmid loss under non-selective conditions (Fig. 9A, track 6). We also prepared protein O-glycans for analysis from the same cultures. Filtered TIM scans of these samples showed that structures corresponding to Xyl-P-Man₂ and Xyl-P-Man₃ increased significantly upon Xpt1 overexpression (Fig. 8, right profiles) and that the magnitude of this change matched the assayed

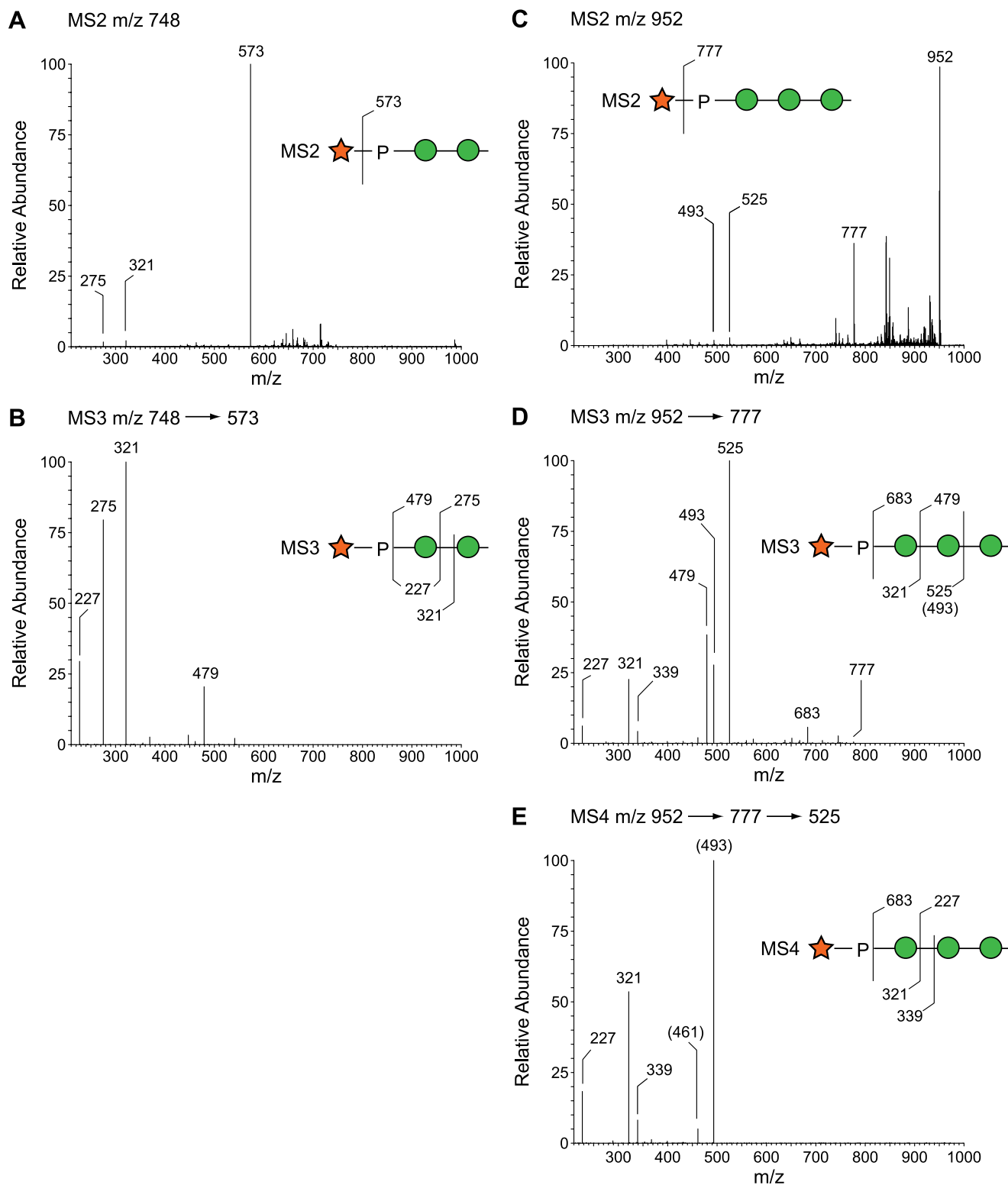


FIGURE 7. Fragmentation of Xyl-P-Man O-glycans in wild type. Panels A and B, the major MS² fragment produced from the parent ion at $m/z = 748$ (Xyl-P-Man₂) corresponds to loss of Xyl ($m/z = 573$). Upon further fragmentation, the $m/z = 573$ ion produces a P-Hex fragment ($m/z = 321$), not a P-hexitol, thereby placing the Xyl-P-substitution at the non-reducing terminus of the Man₂ disaccharide. Panels C–E, similarly, the major MS² fragment produced from the parent ion at $m/z = 952$ (Xyl-P-Man₃) corresponds to loss of Xyl ($m/z = 777$). Further fragmentation produces the P-Hex-Hex ($m/z = 525$) and P-Hex ($m/z = 321$) ions, consistent with Xyl-P-substitution at the non-reducing terminus. The placement of the fragmentation line relative to the indicated residue is meant to indicate cleavage on one side or the other of the glycosidic oxygen.

enzyme activity in all three cultures assessed (Fig. 9B). The absence of detectable Xyl-P modification in the *xpt1Δ* mutant together with the parallel increases in both assayed activity and protein

modification in the overexpression strain strongly support the conclusion that Xpt1p is responsible for Xyl-P modification of mannose in cryptococcal protein O-glycans.

Function of a Cryptococcal Xylosylphosphotransferase

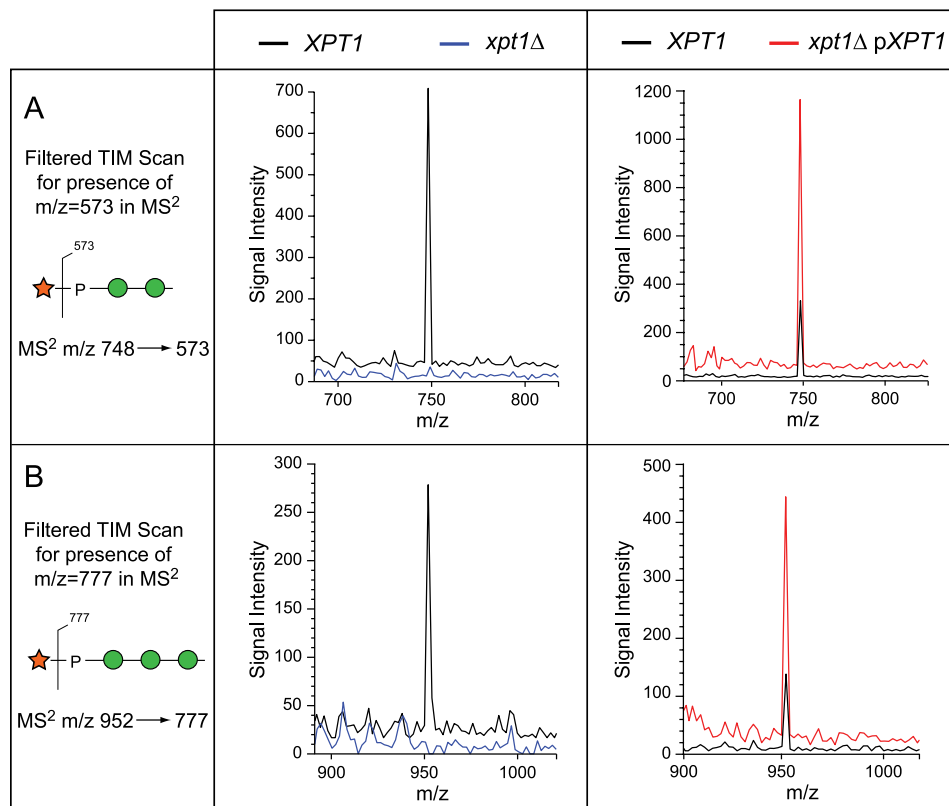


FIGURE 8. Filtered TIM scans demonstrate Xyl-P-Man₂ and Xyl-P-Man₃ in O-linked glycans from wild-type, *xpt1Δ* mutant, and *XPT1* overexpressing strains. Total ion mapping scans were filtered for the production of MS^2 fragments that indicate the presence of Xyl-P motifs (panel A, $m/z = 573$ for Xyl-P-Man₂; panel B, $m/z = 777$ for Xyl-P-Man₃) in the indicated strains. MS^2 is inherently more sensitive than full MS for ion-trap instruments, yet the Xyl-P modified glycans are detected as only minor deflections above base line in the *xpt1Δ* O-linked glycan preparations. The signal traces for KN99 α in the left panels and for *xpt1Δ* p*XPT1* in the right panels are displaced upward on the y axis by 5% of full scale for clarity.

Localization Studies—Although most O-glycosylation of proteins occurs in the endoplasmic reticulum (ER) and Golgi complex (31), there are also important examples of cytosolic O-glycosylation in eukaryotes (32). To localize Xpt1p, we first needed to establish markers for the cryptococcal secretory organelles. The *C. neoformans* genome predicts a protein with 67% homology to *Saccharomyces cerevisiae* BiP, an ER chaperone (33), so we tested this protein as an ER marker. Polyclonal antibody generated against the *S. cerevisiae* protein stained cryptococcal cells in a pattern consistent with the expected ER localization, with fluorescence visible both around the nucleus and just within the plasma membrane (Fig. 10, panels A and B). As a Golgi marker we selected Gmt1p, a GDP-mannose transporter that we previously characterized in *C. neoformans* (34) and showed to functionally complement the corresponding Golgi-localized *S. cerevisiae* protein (Vrg4p). For these studies we used a *C. neoformans* strain where we engineered the chromosomal copy of *GMT1* to express an HA tag.⁶ Localization of this protein exhibited a punctate staining pattern consistent with yeast Golgi localization (35) and distinct from that of the ER marker BiP (Fig. 10, panels A and C).

With these two secretory pathway markers in hand, we proceeded to the localization of Xpt1p. Because immunofluorescence in serotype A strains is technically more challenging,⁷ we

used a serotype D strain (JEC21) episomally expressing either wild-type Xpt1p or the protein modified with a C-terminal HA or FLAG tag. Both untagged and tagged proteins were under control of the same native *XPT1* promoter, and we know that C-terminal epitope tagging does not alter Xpt1p activity (Fig. 1, compare tracks 6 and 8). We observed Xpt1p in a punctate distribution (Fig. 10, panels B and C), highly colocalized with the Gmt1p Golgi protein (Fig. 10, panel C) and clearly distinct from the localization of BiP, the nucleus, and the plasma membrane (Fig. 10, panel B). This suggests that Xpt1p participates in the glycosylation of proteins *en route* through the secretory pathway.

DISCUSSION

We previously identified Xpt1p as a novel glycosyltransferase of *C. neoformans* that modifies Man with Xyl-P (21). In the current study we focused on determining the role of this unusual enzyme. Based on its biochemical activity, we expected Xpt1p to participate in some aspect of cryptococcal glycan synthesis. Although the capsule polysaccharides and glycosylinositol phosphorylceramides of *C. neoformans* are known to include Xyl residues (4, 5, 14), as are the O-glycans of a related cryptococcal species, none of these had been reported to contain a Xyl-P modification. However, the possibility that this unusual structure may have been overlooked in previous analyses together with the lack of definitive structures for many cellular glycans in this organism left open multiple

⁶ C. L. Griffith and T. L. Doering, unpublished data.

⁷ M. L. Skowrya and T. L. Doering, unpublished observations.

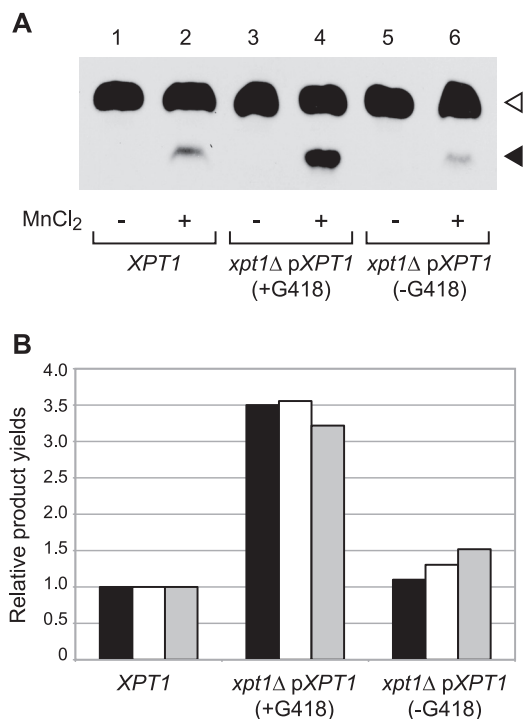


FIGURE 9. Xpt1p overexpression yields parallel increases in enzyme activity and O-glycan modifications. *Panel A*, total membranes were prepared from serotype A wild-type cells or serotype A *xpt1Δ* cells episomally expressing *XPT1* from the same serotype; the latter were cultured either with G418 to maintain the expression plasmid or without it to allow plasmid loss as indicated. Xpt1p activity was assayed with UDP-[¹⁴C]Xyl and α-1,3-Man₂ in the absence (–) or presence (+) of MnCl₂, as described under “Experimental Procedures.” An autoradiograph of the products resolved by TLC is shown; no signal was detected in other regions of the plate beyond minor amounts of free Xyl or in the absence of the α-1,3-Man₂ acceptor (not shown). The filled triangle indicates the product of the manganese-dependent xylosyltransferase activity, and the open triangle indicates the product of the unrelated xylosyltransferase Cxt1P (see “Results”). *Panel B*, shown are Xpt1p products for the strains indicated, normalized to wild-type. Black bars, radiolabel in Xyl-P-Man₂ (filled triangle) made *in vitro* in the reactions shown in panel A, quantified using a BIOSCAN System 200 Imaging scanner; white bars, Xyl-P-Man₂ in protein O-glycans, derived from the abundance of MS² fragments of *m/z* = 573; gray bars, Xyl-P-Man₃ in protein O-glycans, derived from the abundance of MS² fragments of *m/z* = 777.

potential roles for Xpt1p. In the studies reported here we have determined that this enzyme modifies protein O-glycans.

The data presented in Fig. 6 represent our first insights into the structures of O-linked glycans in *C. neoformans*. Beyond the Xyl-P-Man-containing species formed by Xpt1p, we demonstrate the presence of O-linked glycans whose mass is consistent with Man- and Xyl-Man-containing structures. This is significantly different from the O-glycans of the model yeast *S. cerevisiae*, which are composed only of Man residues (36). The Xyl-P-Man motif that we have identified in cryptococcal O-glycans also has not been reported to our knowledge in any system. Phosphate moieties do occur in the O-linked structures of *S. cerevisiae* and *Pichia pastoris* as a terminal modification of mannose (37, 38), but these lack the xylose cap that completes the novel motif found in *C. neoformans*.

The *C. neoformans* species complex diverged into *C. neoformans* (serotypes A and D) and *C. gattii* (serotypes B and C) more than 37 million years ago (39). Genome sequence for

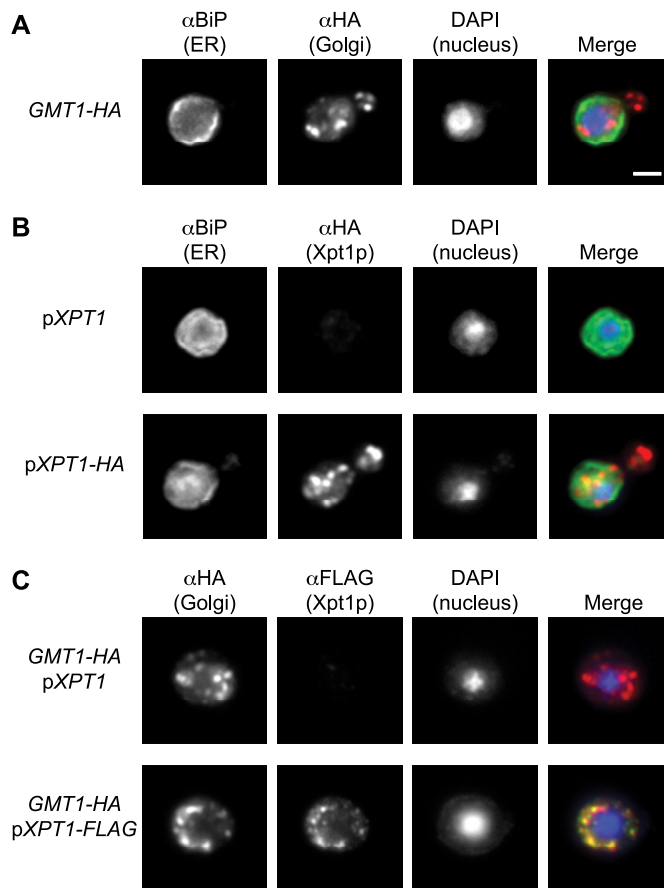


FIGURE 10. Xpt1p-HA localization to the Golgi apparatus. Cryptococcal cells (JEC21) were fixed, permeabilized, immunolabeled, stained with DAPI, and visualized by immunofluorescence microscopy as detailed “Experimental Procedures.” Single channel and merged images are shown. *Panel A*, cells engineered to express an HA-tagged form of Gmt1p (a Golgi marker) were probed with antibodies to BiP (an ER marker) and HA, yielding distinct labeling patterns. *Panel B*, cells episomally expressing either wild-type or HA-tagged Xpt1p were probed with antibodies to BiP and HA, showing distinct labeling patterns. *Panel C*, Gmt1p-HA expressing cells (as in panel A) expressing either wild-type or FLAG-tagged Xpt1p were probed with antibodies to HA and FLAG, showing colocalization. All panels are at the same magnification; scale bar, 2 μm.

strains representing three serotypes (A, B, and D) is available and in each case includes a putative *XPT1* gene; these genes encode proteins that are 88% identical and 92% similar at the amino acid level. The conservation of the region represented by residues 407–456 of Xpt1p in serotype A, which has been implicated in sugar-phosphate transfer from a nucleotide sugar donor (21), is especially notable. The sequences from this region are identical in serotypes A and D, with only a conservative (Ser/Thr) change in serotype B. We tested membranes from nine cryptococcal strains, representing the four serotypes, and found robust Xpt1p activity in all of them (Fig. 2 and data not shown). Furthermore, we showed that expression of *XPT1* from serotype D complements the loss of enzyme activity in a serotype A *xpt1Δ* strain (Fig. 3). Together, these results indicate that both the *XPT1* gene and enzyme activity are highly conserved among members of the *C. neoformans* species complex.

We found no difference between the ability of wild-type and *xpt1Δ* cells to colonize mice, express virulence factors, or grow

Function of a Cryptococcal Xylosylphosphotransferase

under stress conditions. It is conceivable that another protein compensates for loss of Xpt1p via some function that is not measured in our activity assay. This model would account for the lack of detectable phenotypic alteration despite the absence of xylose phosphate transfer activity. One potential candidate is the single *C. neoformans* homolog of Xpt1p, a hypothetical protein that is 35% identical to Xpt1p in serotype A. To test this hypothesis we used RNAi to silence the corresponding gene (CNAG_04705), but we detected no obvious phenotypic change or reduction in Xpt1p activity compared with wild type (21). We also deleted this gene in both wild-type and *xpt1Δ* strains, but neither the single nor double deletion demonstrated any phenotypic change compared with wild-type.⁸ Our working model, therefore, supported by evolutionary conservation, is that Xpt1p performs a necessary function for cryptococcal cells under conditions that are as yet unidentified.

Our understanding of the role of Xpt1p will be informed by identifying specific proteins that are modified by Xpt1p. As seen in Fig. 4, the diffuse Xpt1p-dependent [¹⁴C]Xyl protein labeling that appears between 50 and 100 kDa sometimes resolves into more focused bands (Fig. 4, panel A), but isolating these few highly radiolabeled polypeptides from total membrane sample preparations would be technically challenging. Furthermore, the radiolabeling of membrane proteins in our *in vitro* assay may not accurately represent the native targets of the Xpt1p activity. In the future it may be possible to develop an antibody specific for the Xyl-P-Man motif; this could then be used in the purification and identification of the Xpt1p protein substrates.

We previously showed that a single glycosyltransferase acts in multiple distinct synthetic pathways in *C. neoformans* (19, 20). It is, therefore, possible that Xpt1p modifies *N*-linked glycans in addition to *O*-linked structures. In *S. cerevisiae*, phosphate links mannose residues in some highly mannosylated *N*-glycan structures (40), perhaps serving as precedent for similar structures involving xylose. In another example of phosphate linking two sugar residues, GlcNAc-P is added to terminal mannose residues of mammalian *N*-glycans, although this is followed by removal of the GlcNAc to reveal Man-6-phosphate as a lysosomal targeting signal (41, 42) (we have no evidence for such trimming in the cryptococcal system). Future characterization of cryptococcal *N*-glycans will establish whether they are modified by Xpt1p.

Outstanding questions remain regarding Xpt1p, including the proteins modified by this activity, whether it acts in direct association with other enzymes involved in *O*-glycosylation, and whether it participates in synthesis of *N*-glycans. These investigations will help to define the unusual glycans of *C. neoformans* as well as suggest the biosynthetic pathways required to generate them. Importantly, significant differences in either glycan structure or assembly between this organism and its human host represent potential drug targets for prevention or treatment of cryptococcal infection.

Acknowledgments— We are grateful to Christian Heiss for performing ³¹P NMR studies of GXM and to Mindy Porterfield for protein determinations for glycan analysis. We also thank David Haslam and Jacques Baenziger for helpful insights on this project, Robert Cherniak and Christian Heiss for discussion regarding the structures of GXM and GXMGal, Thomas Kozel for anti-GXM antibodies, and Jeffrey Brodsky for anti-BiP antiserum.

REFERENCES

1. Lin, X., and Heitman, J. (2006) *Annu. Rev. Microbiol.* **60**, 69–105
2. Heitman, J., Kozel, T. R., Kwon-Chung, K. J., Perfect, J. R., and Casadevall, A. (2011) *Cryptococcus, from Human Pathogen to Model Yeast*, pp. 373–385, ASM Press, Washington, D. C.
3. Datta, K., Bartlett, K. H., Baer, R., Byrnes, E., Galanis, E., Heitman, J., Hoang, L., Leslie, M. J., MacDougall, L., Magill, S. S., Morshed, M. G., and Marr, K. A. (2009) *Emerg. Infect. Dis.* **15**, 1185–1191
4. Cherniak, R., Valafar, H., Morris, L. C., and Valafar, F. (1998) *Clin. Diagn. Lab. Immunol.* **5**, 146–159
5. Vaishnav, V. V., Bacon, B. E., O'Neill, M., and Cherniak, R. (1998) *Carbohydr. Res.* **306**, 315–330
6. Heiss, C., Klutts, J. S., Wang, Z., Doering, T. L., and Azadi, P. (2009) *Carbohydr. Res.* **344**, 915–920
7. Samuelson, J., Banerjee, S., Magnelli, P., Cui, J., Kelleher, D. J., Gilmore, R., and Robbins, P. W. (2005) *Proc. Natl. Acad. Sci. U.S.A.* **102**, 1548–1553
8. Olson, G. M., Fox, D. S., Wang, P., Alspaugh, J. A., and Buchanan, K. L. (2007) *Eukaryot. Cell* **6**, 222–234
9. Schutzbach, J., Ankel, H., and Brockhausen, I. (2007) *Carbohydr. Res.* **342**, 881–893
10. Willger, S. D., Ernst, J. F., Alspaugh, J. A., and Lengeler, K. B. (2009) *PLoS One* **4**, e6321
11. Franzot, S. P., and Doering, T. L. (1999) *Biochem. J.* **340**, 25–32
12. Djordjevic, J. T., Del Poeta, M., Sorrell, T. C., Turner, K. M., and Wright, L. C. (2005) *Biochem. J.* **389**, 803–812
13. Eigenheer, R. A., Jin Lee, Y., Blumwald, E., Phinney, B. S., and Gelli, A. (2007) *FEMS Yeast Res.* **7**, 499–510
14. Heise, N., Gutierrez, A. L., Mattos, K. A., Jones, C., Wait, R., Previato, J. O., and Mendonça-Previato, L. (2002) *Glycobiology* **12**, 409–420
15. Rhome, R., McQuiston, T., Kechichian, T., Bielawska, A., Hennig, M., Drago, M., Morace, G., Luberto, C., and Del Poeta, M. (2007) *Eukaryot. Cell* **6**, 1715–1726
16. Moyrand, F., Klaproth, B., Himmelreich, U., Dromer, F., and Janbon, G. (2002) *Mol. Microbiol.* **45**, 837–849
17. Griffith, C. L., Klutts, J. S., Zhang, L., Lavery, S. B., and Doering, T. L. (2004) *J. Biol. Chem.* **279**, 51669–51676
18. Klutts, J. S., Lavery, S. B., and Doering, T. L. (2007) *J. Biol. Chem.* **282**, 17890–17899
19. Klutts, J. S., and Doering, T. L. (2008) *J. Biol. Chem.* **283**, 14327–14334
20. Castle, S. A., Owuor, E. A., Thompson, S. H., Garnsey, M. R., Klutts, J. S., Doering, T. L., and Lavery, S. B. (2008) *Eukaryot. Cell* **7**, 1611–1615
21. Reilly, M. C., Lavery, S. B., Castle, S. A., Klutts, J. S., and Doering, T. L. (2009) *J. Biol. Chem.* **284**, 36118–36127
22. Spiropulu, C., Eppard, R. A., Otteson, E., and Kozel, T. R. (1989) *Infect. Immun.* **57**, 3240–3242
23. Kozel, T. R., Levitz, S. M., Dromer, F., Gates, M. A., Thorikildson, P., and Janbon, G. (2003) *Infect. Immun.* **71**, 2868–2875
24. Eckert, T. F., and Kozel, T. R. (1987) *Infect. Immun.* **55**, 1895–1899
25. Netski, D., and Kozel, T. R. (2002) *Infect. Immun.* **70**, 2812–2819
26. Wickes, B. L., Moore, T. D., and Kwon-Chung, K. J. (1994) *Microbiology* **140**, 543–550
27. Gallagher, S. R. (2006) *Curr. Protoc. Mol. Biol.* Chapter 10, Unit 10.2A
28. Aoki, K., Porterfield, M., Lee, S. S., Dong, B., Nguyen, K., McGlamry, K. H., and Tiemeyer, M. (2008) *J. Biol. Chem.* **283**, 30385–30400
29. Anumula, K. R., and Taylor, P. B. (1992) *Anal. Biochem.* **203**, 101–108
30. Zaragoza, O., and Casadevall, A. (2004) *Biol. Proced. Online* **6**, 10–15
31. Wopereis, S., Lefeber, D. J., Morava, E., and Wevers, R. A. (2006) *Clin.*

⁸ Z. A. Wang and T. L. Doering, unpublished data.

- Chem.* **52**, 574–600
32. Wells, L., and Hart, G. W. (2003) *FEBS Lett.* **546**, 154–158
33. Nishikawa, S., Hirata, A., and Nakano, A. (1994) *Mol. Biol. Cell* **5**, 1129–1143
34. Cottrell, T. R., Griffith, C. L., Liu, H., Nenninger, A. A., and Doering, T. L. (2007) *Eukaryot. Cell* **6**, 776–785
35. Dean, N., Zhang, Y. B., and Poster, J. B. (1997) *J. Biol. Chem.* **272**, 31908–31914
36. Gemmill, T. R., and Trimble, R. B. (1999) *Biochim. Biophys. Acta.* **1426**, 227–237
37. Jars, M. U., Osborn, S., Forstrom, J., and MacKay, V. L. (1995) *J. Biol. Chem.* **270**, 24810–24817
38. Trimble, R. B., Lubowski, C., Hauer, C. R., 3rd, Stack, R., McNaughton, L., Gemmill, T. R., and Kumar, S. A. (2004) *Glycobiology* **14**, 265–274
39. Xu, J., Vilgalys, R., and Mitchell, T. G. (2000) *Mol. Ecol.* **9**, 1471–1481
40. Jigami, Y., and Odani, T. (1999) *Biochim. Biophys. Acta* **1426**, 335–345
41. Kornfeld, S. (1987) *FASEB J.* **1**, 462–468
42. von Figura, K., and Hasilik, A. (1986) *Annu. Rev. Biochem.* **55**, 167–193
43. Nielsen, K., Cox, G. M., Wang, P., Toffaletti, D. L., Perfect, J. R., and Heitman, J. (2003) *Infect. Immun.* **71**, 4831–4841
44. Baker, L. G., Specht, C. A., Donlin, M. J., and Lodge, J. K. (2007) *Eukaryot. Cell* **6**, 855–867
45. Warren, R. L., Butterfield, Y. S., Morin, R. D., Siddiqui, A. S., Marra, M. A., and Jones, S. J. (2005) *Biotechniques* **38**, 715–720
46. Fraser, J. A., Giles, S. S., Wenink, E. C., Geunes-Boyer, S. G., Wright, J. R., Diezmann, S., Allen, A., Stajich, J. E., Dietrich, F. S., Perfect, J. R., and Heitman, J. (2005) *Nature* **437**, 1360–1364
47. Kwon-Chung, K. J., Wickes, B. L., Stockman, L., Roberts, G. D., Ellis, D., and Howard, D. H. (1992) *Infect. Immun.* **60**, 1869–1874